

IIII Development of Boiling and Two-phase Flow Experiments on Board ISS IIII
(Original Paper)

Development of Boiling and Two-Phase Flow Experiments on board ISS (Investigation on Performance of Ground Model)

Tomoki HIROKAWA¹, Daisuke YAMAMOTO¹, Daijiro YAMAMOTO¹, Yasuhisa SHINMOTO¹,
Haruhiko OHTA¹, Hitoshi ASANO², Osamu KAWANAMI³, Koichi SUZUKI⁴, Ryoji IMAI⁵,
Masahiro TAKAYANAGI⁶, Satoshi MATSUMOTO⁶, Takashi KURIMOTO⁶, Hidemitsu TAKAOKA⁶,
Michito SAKAMOTO⁶, Kenichiro SAWADA⁶, Haruo KAWASAKI⁶, Kiyosumi FUJII⁷, Atsushi OKAMOTO⁶,
Kazumi KOGURE⁸, Toshiharu OKA⁹, Toshiyuki TOMOBE⁹ and Koshiro USUSKU⁹

Abstract

Experiments were performed to verify the performance of experimental apparatus for the acquisition of reference data for flow boiling heat transfer under the terrestrial condition which is to be compared with that obtained under the microgravity condition onboard International Space Station (ISS) by using another apparatus with the same specification. Test section is a circular tube made of copper with an inner diameter of 4 mm and a heated length of 368 mm and oriented vertically on ground. To improve the accuracy of local heat fluxes, the compensation of heat flux distribution along the tube axis is discussed on the basis of the experimental results on the local heat transfer coefficients for a single-phase liquid flow. Correlations for local heat transfer coefficient of flow boiling are proposed here as functions of boiling number and Martinelli parameter in the regions of nucleate boiling and two-phase forced convection, respectively. Because the discrepancy of local heat transfer coefficient obtained from the apparatus for the terrestrial and the space experiments is caused by the difference of surface roughness in nucleate boiling region, a compensation factor is introduced in the correlation. The local heat transfer coefficients predicted by the proposed correlation are agreed well with those obtained by both apparatus.

Keyword(s): Flow boiling, Heat transfer, Microgravity, ISS

Received 25 December 2015, Accepted 22 January 2016, Published 31 January 2016

1. Introduction

Boiling and two-phase flow attract much attention for the application to thermal management systems in space craft and/or space platform, where both of power consumption and heat flux density from their equipment are expected to become quite large in near future. However, heat transfer characteristics of boiling and two-phase flow under microgravity (μG) conditions have not been clarified yet in detail because of a limited number of existing data. In order to investigate gravity effect on heat transfer on flow boiling, a series of experiments onboard International Space Station (ISS) is planned by the present authors. One of the most important objectives of the experiment is to clarify the dominant force regime map. Once the gravity-independent regime of operation parameters is clarified, the development and design of the space thermal

management systems can improve their reliability by the iteration of ground tests. For the evaluation of gravity effect on heat transfer of flow boiling, the reference data under the normal gravity condition is important. However, because the experimental apparatus for the operation on orbit, i.e. the flight model has regulations in the experiments under the terrestrial condition (1G). One of the problems is a limitation in a size of working volume of the apparatus. For the evaluation of fundamental heat transfer characteristics of flow boiling, the flow direction in the heated section should not be downward because the instability and corresponding local burnout can occur by the inversed vapor flow due to the buoyancy. For a flight model, because the size of apparatus have to be within the working volume of Multi-purpose Small Payload Rack (MSPR) installed onboard ISS, the layout of tubes avoiding the

1 Kyushu University, 744, Motoooka, Nishi-ku, Fukuoka 819-0385, Japan
2 Kobe University, 1-1, Rokkoudai-chou, Nada-ku, Kobe, Hyogo 657-0013, Japan
3 University of Hyogo, 2167, Shosha, Himeji, Hyogo 671-2201, Japan
4 Tokyo University of Science, Yamaguchi, 1-1-1, Daigakudori, Sanyo-Onoda, Yamaguchi 756-0884, Japan
5 Muroran Institute of Technology, 27-1, Mizumoto-chou, Muroran-shi, Hokkaido 050-8585, Japan
6 Japan Aerospace Exploration Agency, 2-1-1, Sengen, Tsukuba-shi, Ibaraki 305-8505, Japan
7 Nara Institute of Science and Technology, 8916-5, Takayama-chou, Ikoma-shi, Nara 630-0192, Japan
8 Japan Space Forum, 3-2-1, Surugadai, Kanda, Chiyoda-ku, Tokyo 101-0062, Japan
9 IHI Aerospace, 3-1-1, Toyosu, Koutou-ku, Tokyo 135-0061, Japan
(E-mail: hirokawa@aero.kyushu-u.ac.jp)

Table 1 Correlations proposed in the existing reports

Author	Correlation	Fluid Orientation
Sani ³⁾	$\frac{\alpha_{TP}}{\alpha_0} = 1.48[Bo \times 10^4 + 1.5(1/X_{tt})^{2/3}]$	Water Vertical-downward
Wright ⁴⁾	$\frac{\alpha_{TP}}{\alpha_0} = 0.67[Bo \times 10^4 + 3.5(1/X_{tt})^{2/3}]$	Water Vertical-downward
Pujol – Stenning ⁵⁾	$\frac{\alpha_{TP}}{\alpha_0} = 0.90[Bo \times 10^4 + 4.45(1/X_{tt})^{0.37}]$	R113 Vertical-upward
	$\frac{\alpha_{TP}}{\alpha_0} = 0.53[Bo \times 10^4 + 7.75(1/X_{tt})^{0.37}]$	Vertical-downward

downward flow in the experiment under 1G condition cannot be realized. Another problem is the difficulty of the precise adjustment of experimental conditions because of the limitation both in the operation and in the period of experiment onboard ISS. For the accurate evaluation of gravity effect on flow boiling heat transfer, the experiments on ground should be conducted after those onboard ISS because the experimental conditions on ground can be more accurately adjusted. Then, the reference data of flow boiling heat transfer should be obtained by using another apparatus. In order to compare with the experimental results obtained by different apparatus, the difference of data caused by the structure and/or the surrounding thermal environments have to be clarified in advance. First of all, the verification of performance of the components integrated in the flight model (FM) is needed. Present authors designed Ground Model (GM) for the acquisition of reference data on ground, where the components which have the same specifications as those in the flight model are introduced. In the present paper, experiments were conducted to verify the performance of GM and to establish a correlation for local heat transfer coefficients of flow boiling on ground. To fill the gap of local heat transfer coefficients of flow boiling obtained between GM and FM, the process of compensation of local heat transfer coefficients is discussed by using the results obtained by Proto Flight Model (PFM) with the same components and layout of tubes with FM.

Heat transfer characteristics of flow boiling in a circular tube under 1G condition have been investigated and the correlations of heat transfer coefficient were proposed in a number of researchers. The correlations of heat transfer coefficient for flow boiling were proposed as empirical correlations for vertical-upward flow of water in 1 inch circular tube by Dengler and Addoms¹⁾. In their correlation, the terms of the Dittus-Boelter equation α_0 , Martinelli parameter X_{tt} and a constant F_{DA} are introduced as follows.

$$\frac{\alpha_{TP}}{\alpha_0} = 3.5 \frac{F_{DA}}{X_{tt}^{0.5}}, \quad (1)$$

$$\alpha_0 = 0.023 \frac{\lambda_l}{D} \left(\frac{GD}{\mu_l} \right)^{0.8} \left(\frac{c_{p,l} \mu_l}{\lambda_l} \right)^{0.4},$$

where D is a diameter of tube, λ_l is a thermal conductivity of liquid, G is a mass velocity, μ_l is a dynamic viscosity of liquid and $c_{p,l}$ is a specific heat of liquid. Similarly, a number of researchers proposed the correlation of local heat transfer coefficient of flow boiling as a function of Martinelli parameter. Schrock and Grossman²⁾ proposed the correlation taking account of nucleate boiling and two-phase forced convection as a function of Boiling number and Martinelli parameter for vertical-upward flow of water.

$$\frac{\alpha_{TP}}{\alpha_0} = 0.739[Bo \times 10^4 + 1.5(1/X_{tt})^{2/3}], \quad (2)$$

$$Bo = \frac{q}{Gh_{fg}},$$

where h_{fg} is a latent heat. Some researchers proposed correlations for the heat transfer coefficients covering those of nucleate boiling to those of two-phase forced convection as shown in **Table 1**. Chen⁶⁾ established a heat transfer model taking account of heat transfer in micro region, where boiling played an important role, and that in macro region, where heat transfer is influenced by forced convection based on a lot of existing experimental investigations. Kandlikar⁷⁾ summarized the data of heat transfer coefficient and proposed the correlations for flow boiling in horizontal and vertical tubes. His correlation was as a function of parameter F_{ff} dependent of fluid, Froude number in the case of the total flow as liquid F_{rlo} and convection number, Boiling number. Later, the correlation was refined with reference to 24 experimental investigations⁸⁾.

To verify the performance of GM, a correlation of local heat transfer coefficient for flow boiling is established as a function of Boiling number in nucleate boiling region and Martinelli parameter in the region of two-phase forced convection. In addition, for accurate evaluation of heat transfer coefficients, the estimation of heat loss and the compensation of heat flux distribution in the longitudinal direction are discussed on the basis of the local heat transfer coefficients due to single-phase forced convection.

2. Experimental Apparatus

Figure 1 shows a test loop for Ground Model (GM). The main components of GM have the same specification as those of FM. In addition, in order to reduce the difference of heat loss by the heat conduction in the longitudinal direction between GM and FM, the lengths of tubes connecting the components are

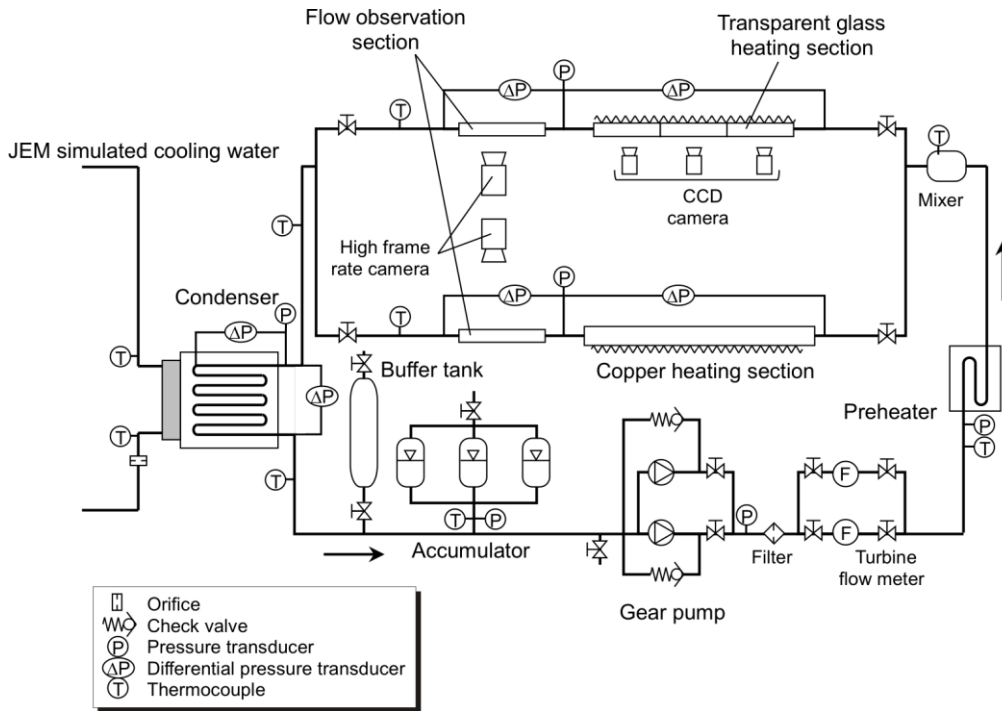


Fig. 1 Test loop.

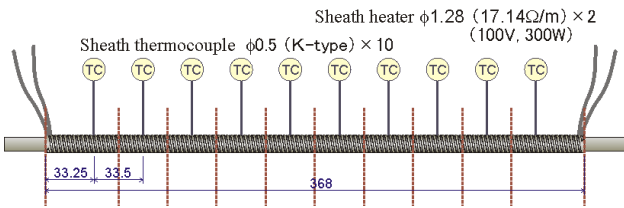


Fig. 2 Metal heated tube.

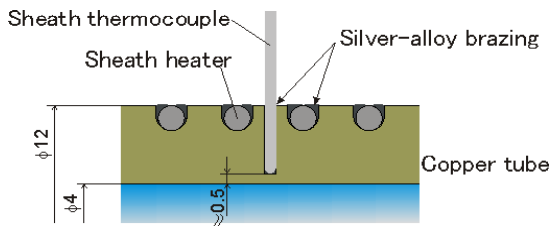


Fig. 3 Structure of cross section in metal heated tube.

adjusted to be the same. Two pumps and two flow meters are installed and switched by valves to extend the experimental range of flow rates without oscillation. For high flow rates ($G > 100 \text{ kg}/(\text{m}^2\text{s})$), the combination of the pump (Micropump 185 GA-V23J8FSA) and the turbine flow meter (FTO-2NIXSULHC-1) are selected, while, the combination of the pump (Micropump 187 GA-X21J8FSA) and the turbine flow meter (FTO-1 NIXSBLHC-1) are used for low flow rates ($G < 100 \text{ kg}/(\text{m}^2\text{s})$). A preheater is introduced for the control of

the inlet subcooling or quality. Two vertical test sections located in parallel are switched by valves. One of the test section is a metal heated tube as shown in Fig. 2. By using the metal heated tube, local heat transfer coefficients and critical heat fluxes are evaluated. The tube is made of copper with an inner diameter of 4 mm and a heated length of 368 mm. The sheath heaters are coiled around the grooves on the outer tube wall as shown in Fig. 3. The groove is filled with silver brazing to decrease the heat resistance and realize uniform heat flux on the inner tube wall. To measure wall temperature distribution along the flow direction, ten thermocouples are located at 33.5 mm intervals. Each thermocouple is inserted into the tube in the radial direction and located at a distance of 0.5 mm from the inner wall. The other test section is a transparent heated tube. The

Table 2 Experimental conditions.

	PFM	GM
Power supply to heaters	$Q_{total} < 250 \text{ W}$	
Test fluid	n-perfluorohexane	FC72
Inner diameter of heated sections	$d_i = 4 \text{ mm}$	
Heated length	$l = 368 \text{ mm}$	
Mass velocity	$G = 30\text{--}300 \text{ kg}/(\text{m}^2\text{s})$	
Inlet liquid subcooling	$\Delta T_{sub} = 0\text{--}30 \text{ K}$	
Inlet quality	–	$x = 0\text{--}0.7$
Heat flux	$q < 26 \text{ kW}/\text{m}^2$	

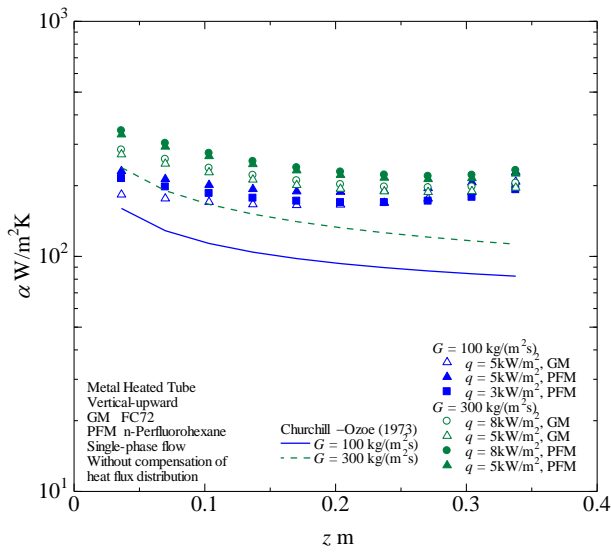


Fig. 4 Local heat transfer coefficient along the flow direction without compensation of heat flux distribution.

tube is made of Pyrex glass with an inner diameter of 4 mm. A thin gold film is coated uniformly on the inner wall. Heat flux is given by the electric heating of the thin gold film. The averaged inner wall temperature at each segment is measured by the electric resistance varied with its temperature. The gold film is thin enough to observe the liquid-vapor behaviors inside of the glass tube through the wall by CCD cameras. The tube is divided into three segments along the flow direction to evaluate three local heat transfer coefficients. The heated length is 50 mm for the 1st and 2nd segments and 5 mm for the 3rd segment, respectively. The shortest heated tube can detect the temperature fluctuation corresponding to the transition of interfacial behaviors at e.g. CHF conditions. In the downstream of each test section, an unheated test section is connected for the observation of detailed liquid-vapor behaviors by a high-speed video camera (IDT MotionXtra N3) operated at 1000 fps. A condenser is introduced to obtain the steady-state data by the removal of the same amount of heat supplied by the pre-heater and the heated test section. The condenser has 8 tube passes made of copper and the outer wall temperature distribution along the flow direction is measured by thermocouples. A cooling systems simulating JEM cold water loop is employed to condense the test fluid and give it the subcooling to prevent the pump cavitation. The accumulator is introduced for the adjustment of pressure in the loop by controlling back pressure. Experimental conditions are shown in **Table 2**. In FM, the amount of the total heater power is limited up to 250 W. In addition, the inlet conditions of $x_{in} > 0$ were not conducted by using FM for avoiding the downward flow in the pre-heater. Test fluid is used n-perfluorohexane, while test fluid in GM is FC72 whose main component is n-perfluorohexane. All of the measurement

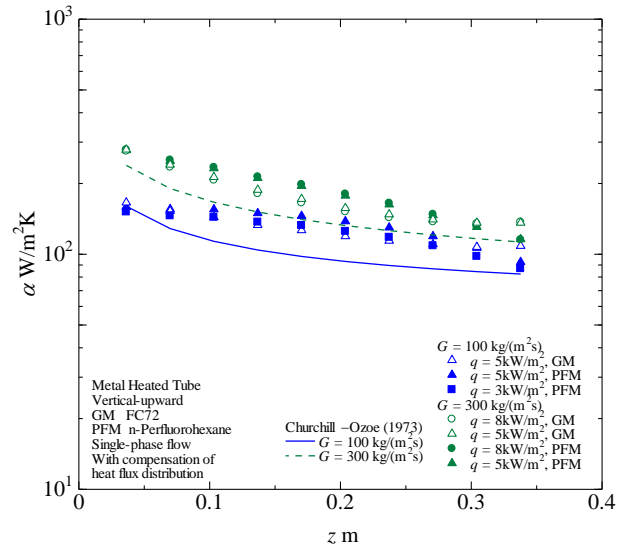


Fig. 5 Local heat transfer coefficient along the flow direction with compensation of heat flux distribution.

systems are carefully calibrated. The uncertainties are ± 0.15 K in the measured temperature, ± 2 %FS in pressure, ± 0.25 %RD in flow rate and ± 0.1 %RD in heat flux.

3. Compensation of heat flux distribution

In order to evaluate the heat flux distribution along the flow direction compensating the heat loss, the local heat transfer coefficient for single-phase liquid is discussed here. The local heat transfer coefficient is defined as follows.

$$\alpha_i = \frac{q_i}{T_{w,i} - T_{l,i}}, \quad (3)$$

where q_i is a local heat flux, $T_{w,i}$ is a local wall temperature and $T_{l,i}$ is a local liquid mean temperature. Liquid bulk temperature is assumed to increase linearly between the measured values at the inlet and outlet of the heated test section. **Figure 4** shows local heat transfer coefficients along the flow direction in the laminar flow region under various combinations of mass velocities and heat fluxes experimented in GM and the proto flight model (PFM). The critical Reynolds number corresponding to the onset of turbulence ($Re_D=2300$) is given by the mass velocity of 390 kg/(m²s) for an inner diameter of 4 mm. The predicted value by Churchill – Ozoe correlation for laminar flow⁹⁾ is also shown in the figure. In Churchill – Ozoe correlation, the local heat transfer coefficient which takes account of development of thermal boundary layer from the inlet is described.

$$\alpha_z = 5.364 \frac{\lambda_f}{D} \left[1 + \left(\frac{220z/D}{\pi Re_D Pr} \right)^{-1.11} \right]^{0.3} - 1, \quad (4)$$

where z is a distance from the entrance of heated section and D is a diameter. The local heat transfer coefficients obtained from PFM and GM become larger at higher mass velocity and are independent of heat flux, which is consistent with the general trends in single-phase liquid flow with constant thermal properties. However, the trend of the increase of local heat transfer coefficient towards the downstream is not agreed with the correlation. Moreover, the level of local heat transfer coefficients obtained by PFM is larger than those obtained by GM. These disagreement seems to be caused by the ignorance of heat loss from the edges in the longitudinal directions. In order to obtain the accurate heat flux distribution along the tube wall, the compensation of heat loss was performed as follows. Firstly, on the cylindrical surface involving the bottom of grooves in **Fig. 3**, the uniform heat flux evaluated from the power input is assumed. Secondly, the temperature distribution along the inner wall in the direction of tube axis is estimated by polynomial approximation using measured local wall temperatures. At the both edges of the tube along the flow direction, the heat loss is evaluated by the heat conduction with reference to the measured inner wall temperature gradient between the 1st and 2nd segments and between the 9th and 10th segments. By using these boundary conditions, steady-state heat conduction in the tube wall is solved to obtain the heat flux distribution along the axis.

Figure 5 shows the local heat transfer coefficients along the flow direction with compensation of heat flux distribution. The local heat transfer coefficient towards the downstream for all combinations of mass velocities and heat fluxes is decreased, which agrees with the trend of the correlation. In addition, the discrepancy of heat transfer coefficients between PFM and GM is decreased from the results shown in **Fig. 4**. However, the levels of heat transfer coefficients obtained in PFM and GM at the midstream are larger than those predicted by the correlation, which is due to the overestimation of heat flux neglecting the heat loss from the outer wall to the material of thermal insulation. For further improvement of accuracy on estimation of local heat fluxes, the evaluation of heat loss from the outer wall is needed.

Figure 6 shows the comparison of Nusselt numbers between experimental values in turbulent region at all segments and those predicted by correlations proposed by Duttus – Boelter¹⁰ and Colburn¹¹. The experimental values in the figure are compensated by the heat loss to the axial direction. With compensation of heat flux distribution, the scattering of Nusselt number in the longitudinal axis is decreased. The Nusselt number based on the experimental data is agreed with those

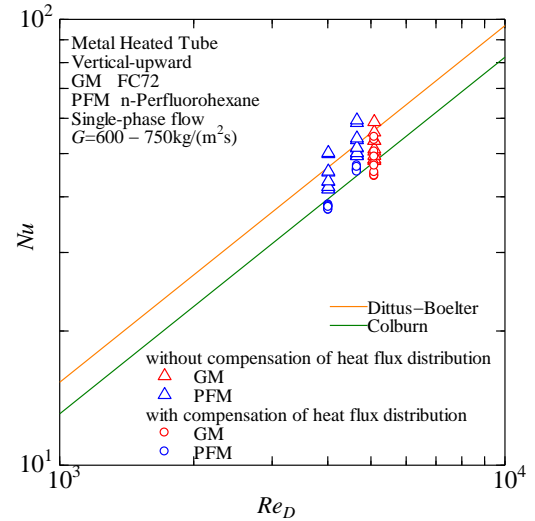


Fig. 6 Relationship between Nusselt number and Reynolds number in turbulent region.

predicted by the correlation of Colburn. The experimental data of single-phase flow indicates that the heat loss compensation along the flow direction is valid for the improvement of accuracy in the evaluation of local heat transfer coefficients for flow boiling.

4. Local heat transfer coefficient for flow boiling

Local heat transfer coefficient is defined by Eq. (3). The liquid temperature at the locations in the two-phase region is assumed to be the saturation temperature corresponding to the pressure at the outlet of the heated test section.

Figure 7 shows the relationship between the local heat transfer coefficient and quality obtained by GM at mass velocity of 300 kg/(m²s). The broken lines and the red circle are indicated for the values predicted by the correlation in the present paper, which are discussed in the later section. In the low quality region, the local heat transfer coefficient is not changed with increasing quality. In addition, the local heat transfer coefficient is increased with increasing heat flux. These trends observed in the low quality region are agreed with those of nucleate boiling heat transfer. In the high quality region, the local heat transfer coefficient becomes larger at higher quality, while the local heat transfer coefficient is independent of heat flux. The trends are agreed with those of two-phase forced convective heat transfer.

Figure 8 shows the relationship between the local heat transfer coefficient and quality obtained by PFM at mass velocity of 300 kg/(m²s). In PFM, the local heat transfer coefficients under the conditions of low heat flux and high quality cannot be obtained because the experiments of quality region at the inlet were not conducted to avoid instability caused by the downward flow in the preheater. In addition, the experiments at mass

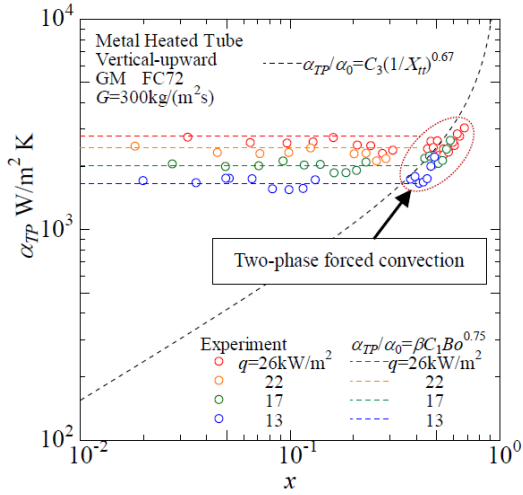


Fig. 7 Local heat transfer coefficient versus quality at $G=300 \text{ kg}/(\text{m}^2\text{s})$ obtained by GM.

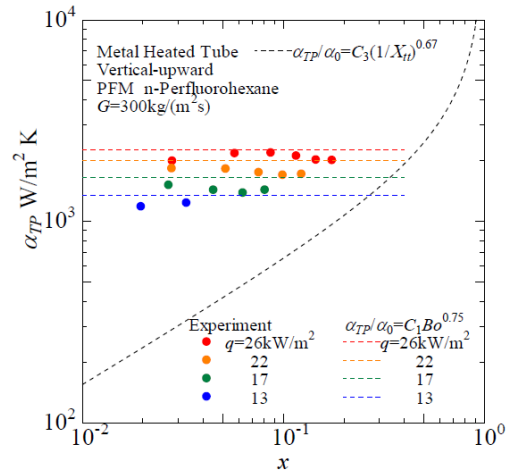


Fig. 8 Local heat transfer coefficient versus quality at $G=300 \text{ kg}/(\text{m}^2\text{s})$ obtained by PFM.

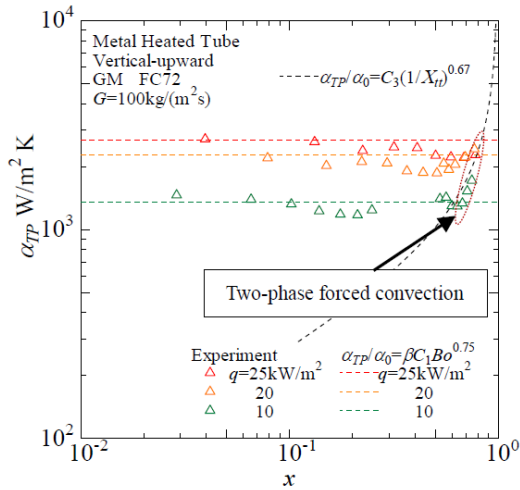


Fig. 9 Local heat transfer coefficient versus quality at $G=100 \text{ kg}/(\text{m}^2\text{s})$ obtained by GM.

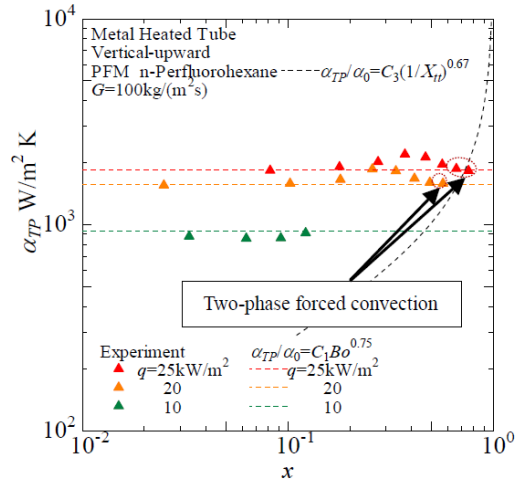


Fig. 10 Local heat transfer coefficient versus quality at $G=100 \text{ kg}/(\text{m}^2\text{s})$ obtained by PFM.

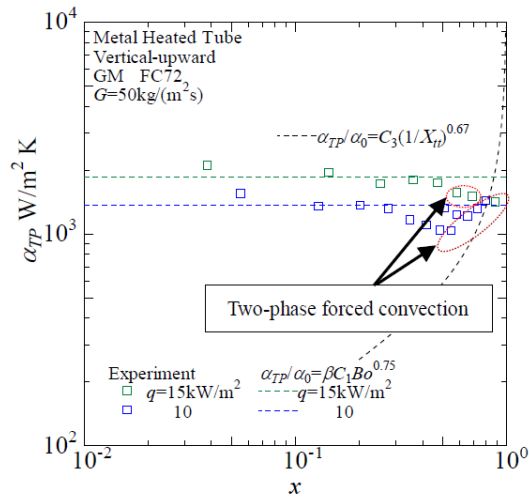


Fig. 11 Local heat transfer coefficient versus quality at $G=50 \text{ kg}/(\text{m}^2\text{s})$ obtained by GM.

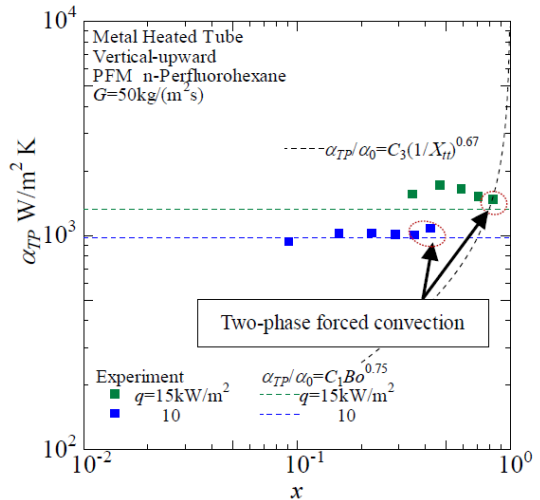


Fig. 12 Local heat transfer coefficient versus quality at $G=50 \text{ kg}/(\text{m}^2\text{s})$ obtained by PFM.

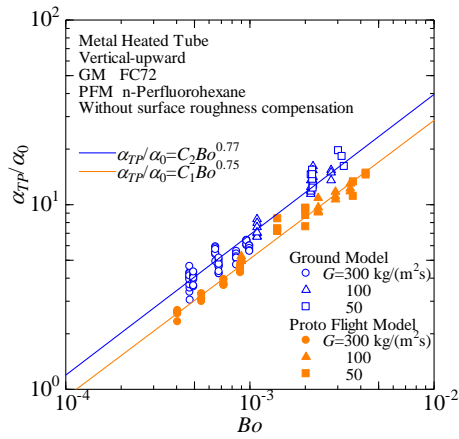


Fig. 13 The value of α_{TP}/α_0 versus Boiling number Bo obtained by GM and PFM.

velocity of 300 kg/(m²s) in the high quality region cannot be conducted because of the limitation of heater power below 250 W. In the low quality region, the heat transfer coefficient becomes larger at higher heat flux as already described before. However, the levels of local heat transfer coefficient obtained by GM are larger than those obtained by PFM because the surface roughness is influenced generally in nucleate boiling heat transfer. In the high quality region, it is well known that the values of local heat transfer coefficient due to two-phase forced convection are not influenced by the surface conditions. **Figure 9** shows the relationship between the local heat transfer coefficient and quality obtained by GM at mass velocity of 100 kg/(m²s). In the low quality region, the trends for the influence of heat flux and quality on the heat transfer coefficient due to nucleate boiling is similar to those for 300 kg/(m²s). At this mass velocity, the local heat transfer coefficients due to two-phase force convection are also obtained in the high quality region. **Figure 10** shows the results obtained by PFM at mass velocity of 100 kg/(m²s). No distinct trend of the local heat transfer coefficient in the high quality region can be observed because of the limitation in the experimental condition inherent in PFM. The levels of the local heat transfer coefficient obtained by GM are also larger than those obtained by PFM. **Figure 11** shows the data obtained by GM at 50 kg/(m²s). In both of high and low quality regions, the trends of local heat transfer coefficient are agreed with those observed at mass velocities of 300 and 100 kg/(m²s). **Figure 12** shows the data by PFM at 50 kg/(m²s). The difference of local heat transfer coefficient obtained between GM and PFM becomes smaller than those at 300 and 100 kg/(m²s). For the evaluation of local heat transfer coefficient under 1G condition as the reference data for the data under μ G condition, a correlation of local heat transfer coefficient from the results obtained by both of GM and PFM is established below. In the low quality region, to take account of

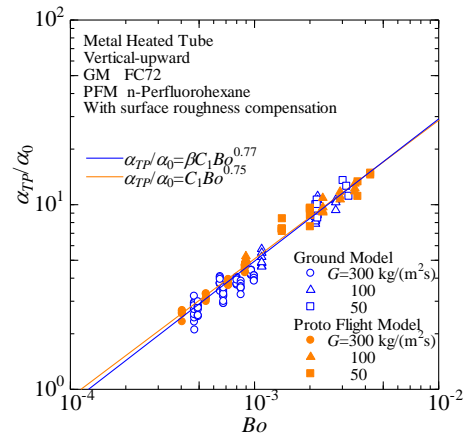


Fig. 14 The value of α_{TP}/α_0 versus Boiling number Bo obtained by GM and PFM with surface roughness compensation.

the trend of nucleate boiling heat transfer, Boiling number Bo is introduced. In addition, for GM, a constant correction factor β is introduced to fill the gap of local heat transfer coefficients due to nucleate boiling obtained from GM and PFM. The difference of heat transfer coefficients is caused by the different surface conditions, e.g. surface roughness.

For PFM

$$\frac{\alpha_{TP}}{\alpha_0} = C_1 Bo^n. \quad (5)$$

For GM

$$\frac{\alpha_{TP}}{\alpha_0} = \beta C_1 Bo^n = C_2 Bo^n, \quad (6)$$

where α_0 is a heat transfer coefficient obtained by Dittus-Boelter equation in the case of the total flow as liquid. In high quality region, in order to take account of the trend of two-phase forced convective heat transfer, Martinelli parameter $1/X_{tt}$ is introduced as follows.

$$\frac{\alpha_{TP}}{\alpha_0} = C_3 \left(\frac{1}{X_{tt}} \right)^m, \quad (7)$$

$$\frac{1}{X_{tt}} = \left(\frac{x}{1-x} \right)^{0.9} \left(\frac{\rho_l}{\rho_g} \right)^{0.5} \left(\frac{\mu_g}{\mu_l} \right)^{0.1}.$$

The heat transfer data which is regarded to have the trends of two-phase forced convective region are selected tentatively by a red circle shown in **Fig. 7** and **Figs. 9 – 12**.

Figure 13 shows the relationship between α_{TP}/α_0 and Bo in nucleate boiling region obtained by both models of experimental setup. From the least-square method, the value of $C_1=1200$ and $C_2=850$ are obtained. α_{TP}/α_0 has a function of $Bo^{0.77}$ for GM,

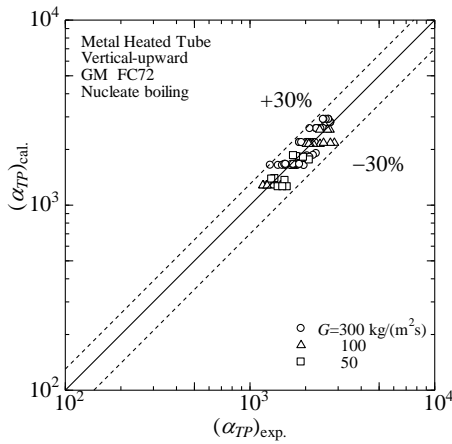


Fig. 15 Comparison between the local heat transfer coefficient predicted by the correlation of $\alpha_{TP}/\alpha_0 = \beta C_1 Bo^{0.75}$ and those obtained by experiment in GM.

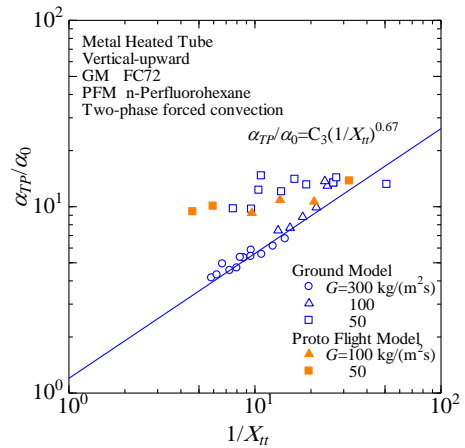


Fig. 17 The value of α_{TP}/α_0 versus Martinelli parameter $1/X_{tt}$ obtained by GM and PFM.

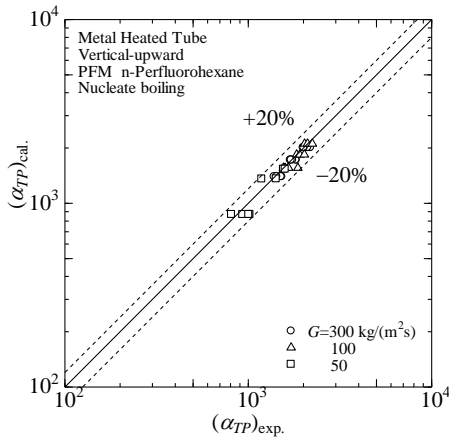


Fig. 16 Comparison between the local heat transfer coefficient predicted by the correlation of $\alpha_{TP}/\alpha_0 = C_1 Bo^{0.75}$ and those obtained by experiment in PFM.

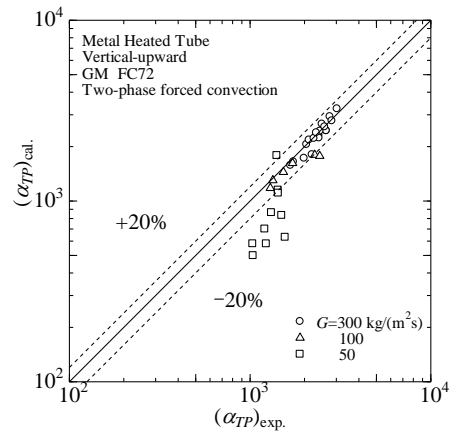


Fig. 18 Comparison between the local heat transfer coefficient predicted by the correlation of $\alpha_{TP}/\alpha_0 = C_3(1/X_{tt})^{0.67}$ and those obtained by experiment in GM.

which is well agreed with that of $Bo^{0.75}$ for PFM. Moreover, the similar trends are obtained at different mass velocities in each setup model. **Figure 14** shows the comparison of α_{TP}/α_0 versus Bo after the compensation of surface roughness. The results indicate that the compensation of surface roughness effect is valid for α_{TP}/α_0 in nucleate boiling region. The local heat transfer coefficient by the calculation and by the experiments in nucleate boiling region are compared for GM and PFM, as shown in **Figs. 15** and **16**, respectively. The correlation is well agreed with the experimental results within an error of $\pm 30\%$ for GM and within an error of $\pm 20\%$ for PFM, respectively.

Figure 17 shows α_{TP}/α_0 versus Martinelli parameter ($1/X_{tt}$) for two-phase forced convection. Because the limited number of heat transfer data was obtained in PFM owing to the regulation of the experimental apparatus under 1G condition, the

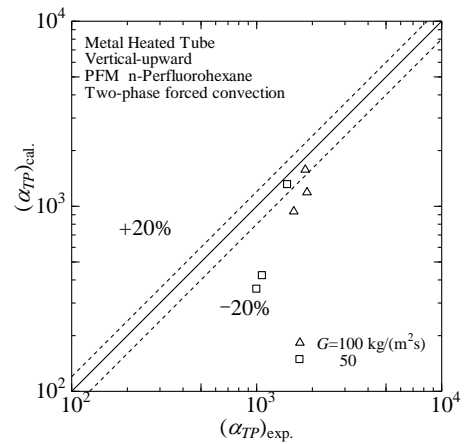


Fig. 19 Comparison between the local heat transfer coefficient predicted by the correlation of $\alpha_{TP}/\alpha_0 = C_3(1/X_{tt})^{0.67}$ and those obtained by experiment in PFM.

correlation is derived only in the case of GM. From the results of calculation of least-square method, the value of $C_3=1.2$ is obtained. α_{TP}/α_0 has a function of $(1/X_{tt})^{0.67}$. For GM, the correlation is well agreed with the experimental data with an error of $\pm 30\%$ except that at mass velocity of 50 kg/(m²s). At this mass velocity, the trend of heat transfer seems to be that of nucleate boiling because the value of α_{TP}/α_0 is insensitive to $1/X_{tt}$. For PFM, all data at mass velocities of 100 and 50 kg/(m²s) is of nucleate boiling. The local heat transfer coefficient by the calculation versus those by the experiments in two-phase convective region is plotted for GM and PFM in **Figs. 18** and **19**, respectively. For GM, the correlation is agreed with the experimental data within an error of $\pm 20\%$ except the data at mass velocity of 50 kg/(m²s), which seems to have the trend of nucleate boiling as was confirmed in **Fig. 17**. For PFM, the correlation is not agreed at all with the experimental data because the data tentatively regarded as that of two-phase forced convection seems to be of nucleate boiling.

For the confirmation of the validity of the proposed correlations for local heat transfer coefficient in the entire quality region, the calculated values by the correlations are represented by broken lines for each mass velocity in **Figs. 7 – 12**. The experimental data of local heat transfer coefficient obtained by GM is well predicted by Eqs. (6) and (7) in the entire quality region at mass velocities of 300 and 100 kg/(m²s) as shown in **Figs. 7** and **9**, respectively, while the data at mass velocity 50 kg/(m²s) is agreed with Eq. (6) as shown in **Fig. 11**. On the other hand, the data obtained by PFM is well predicted by Eq. (5) in the experimental range of quality at 300, 100 and 50 kg/(m²s) as shown in **Figs. 8, 10** and **12**, respectively.

5. Conclusions

To confirm the accuracy of reference data of flow boiling heat transfer under the terrestrial condition to be compared with that obtained under microgravity conditions, local heat transfer coefficients by two test sections integrated in the ground model and the proto flight model were examined, at mass velocity varied from 50 to 300 kg/(m²s) and heat flux increased up to 26 kW/m² for vertical-upward flows on ground. The followings were clarified.

1. From the experimental results of local heat transfer coefficient for single-phase flow, the compensation of heat flux distribution in the flow direction by using wall temperature distribution was performed, which were valid for both of laminar and turbulent flow.
2. In the nucleate boiling region, a proposed correlation as a function of Boiling number was agreed with the experimental results obtained by each model within an error of $\pm 30\%$ for the ground model and within an error of $\pm 20\%$ for the proto flight model, respectively.
3. The gap of local heat transfer coefficients caused by the difference of surface roughness between the test sections integrated in the proto flight model and the ground model was filled successfully by introducing a compensation factor.
4. In the two-phase forced convective region, a correlation as a function of Martinelli parameter was agreed with experimental results obtained by the ground model, while there was no heat transfer data due to two-phase forced convection obtained by the proto flight model because of the restriction in the experimental quality range to avoid the downward flow of liquid-vapor mixtures on the ground. In the space experiment, the data acquisition at higher quality became possible under the condition of positive quality at the inlet of heated test section.

It was concluded that the ground model was valid for the acquisition of reference heat transfer data under the terrestrial condition to be used for the comparison with that obtained under microgravity conditions onboard ISS.

References

- 1) C.E. Dengler and J.N. Addoms: Chemical Engineering Progress Symposium Series, **52** (1956) 95.
- 2) V.E. Schrock and L.M. Grossman: Nuclear Science and Engineering, **12** (1962) 474.
- 3) R.L. Sani: United States Atomic Energy Commission Report UCRL-10527 (1960).
- 4) R.M. Wright: United States Atomic Energy Commission Report UCRL-9744 (1961).
- 5) L. Pujor and A.H. Stenning: Symposium Series of the Canadian Society for Chemical Engineering, Plenum Press N. Y., **1** (1969) 401.
- 6) J.C. Chen: Industrial and Engineering Chemistry, Process Design and Development, **5** (1966) 322.
- 7) S.G. Kandlikar: American Society of Mechanical Engineers, (1983).
- 8) S.G. Kandlikar: American Society of Mechanical Engineers Journal of Heat Transfer, **112** (1990) 219.
- 9) S.W. Churchill and H. Ozoe: Journal of Heat Transfer, **95** (1973) 78.
- 10) F.W. Dittus and L.M.K. Boelter: University of California Publications in Engineering, **2** (1930) 443.
- 11) A.P. Colburn: Transactions of the American Institute of Chemical Engineers, **29** (1933) 174.